TECHNICAL REPORT ARBRL-TR-02242

SHEAR STRAINS, STRAIN RATES AND TEMPERATURE CHANGES IN ADIABATIC SHEAR BANDS

Gerald L. Moss

May 1980

US ARMY ARMAMENT RESEARCH AND DEVELOPMENT COMMAND
BALLISTIC RESEARCH LABORATORY
ABERDEEN PROVING GROUND, MARYLAND

UNCLASSIFIED

SECURITY CLASSIFICATION OF THIS PAGE (When Data Entered)

REPORT DOCUMENTATION PAGE	READ INSTRUCTIONS BEFORE COMPLETING FORM
1. REPORT NUMBER TECHNICAL REPORT ARBRL-TR-02242	2. GOVT ACCESSION NO. AD-A087765	3. RECIPIENT'S CATALOG NUMBER
4. TITLE (and Subtitle) Shear Strains, Strain Rates and Temperature Changes in Adiabatic Shear Bands		5. TYPE OF REPORT & PERIOD COVERED
		6. PERFORMING ORG. REPORT NUMBER
7. AUTHOR(s) Gerald L. Moss		8. CONTRACT OR GRANT NUMBER(s)
9. PERFORMING ORGANIZATION NAME AND ADDRESS US Army Ballistic Research Laboratory ATTN: DRDAR-BLT Aberdeen Proving Ground, MD 21005		10. PROGRAM ELEMENT, PROJECT, TASK AREA & WORK UNIT NUMBERS Proj. Element 6.11.02A DA Proj. No. 1L161102AH43 AMCMS Code 611102.H4300
11. CONTROLLING OFFICE NAME AND ADDRESS US Army Armament Research & Development Command US Army Ballistic Research Laboratory(DRDAR-BL) Aberdeen Proving Ground, MD 21005		12. REPORT DATE May 1980 13. NUMBER OF PAGES 30
14. MONITORING AGENCY NAME & ADDRESS(if different from Controlling Office)		15. SECURITY CLASS. (of this report) Unclassified 15c. DECLASSIFICATION/DOWNGRADING SCHEDULE N/A

16. DISTRIBUTION STATEMENT (of this Report)

Approved for public release; Distribution unlimited.

17. DISTRIBUTION STATEMENT (of the abstract entered in Block 20, if different from Report)

18. SUPPLEMENTARY NOTES

19. KEY WORDS (Continue on reverse side if necessary and identify by block number)

Adiabatic shear, thermoplastic, plasticity, plastic deformation, armor, steel

20. ABSTRACT (Continue on reverse side if necessary and identify by block number) bet/2972

Experiments were conducted to determine the shear strains and strain rates in adiabatic shear bands in a Ni-Cr steel (rolled armor). An explosively driven mass was used to punch plugs from plates of the steel and, thereby, create adiabatic shear bands. There were originally planes of chemical inhomogeneity (reference bands) in the plane of the steel samples. The slopes of the reference bands were altered by the plastic shear, and they were, therefore, a measure of the plastic shear strain. From measurements of the slopes of the

(OVER)

reference bands, it was found that the plastic shear was approximately an exponential function of distance through an adiabatic shear band. Shear strains of at least 572 developed after the onset of adiabatic shear, and with measured rates of punching, it was estimated that shear strain rates as great as 9.4×10^{7} sec^{-1} were attained within the adiabatic shear bands. The results suggest how heating occurs within the shear bands, the maximum temperatures attained and the related strength degradation associated with the development of an adiabatic shear band.

TABLE OF CONTENTS

I. INTRODUCTION

Phenomenological investigations of the rapid plastic deformation of metals have generally revealed that the deformation is inhomogeneous and concentrated in narrow shear bands. For example, metallographic observations have revealed regions of concentrated shear in explosively fragmented shells, machining chips and impacted plates and projectiles. Typical examples[1,2] are shown in Fig. 1.

In the 1940's, Zener[3] suggested that the heat created in plastic working would remain concentrated in, or near, shear bands whenever the heat is created more quickly than it can be removed by conduction. He also noted that the strength of many materials decreases with increasing temperature, and he proposed, therefore, that when materials of this type are deformed rapidly enough for the occurrence of localized heating, the process should lead to catastrophic failure at the shear bands.

Later, Recht proposed a mathematical model to describe the temperature T of an infinitely thin shear band.[4] He found that for such a band the temperature attained should depend expicitly on the local values of the strain γ and strain rate $\dot{\gamma}$ according to the relation

$$T = \frac{\tau_y}{J}\left[\frac{\dot{\gamma}(\gamma-\gamma_y)}{\pi K\rho C}\right]^{\frac{1}{2}}, \qquad (1)$$

where τ_y and γ_y are the yield stress and strain respectively in shear, J is the mechanical equivalent of heat, K is the thermal conductivity, ρ is the density, C is the specific heat, and γ and $\dot{\gamma}$ are the shear strain and strain rate respectively on the shear plane.

In reality, shear bands always occur with a finite thickness, and in this event, the temperature of the sheared material also depends on the width of the shear band since heat must be conducted through this distance. This, however, does not change the main features of what Recht originally proposed, i.e., that the heating of the shear zone depends on the plastic strain, the plastic strain rate and the rate at which heat is conducted away from the shear zone.

---

[1] *K. C. Dao and D. A. Shockey, "A Method for Measuring Shear Band Temperatures," J. Applied Phys., Vol. 50, No. 12, December 1979, pp. 8244-6.*

[2] *W. Braerman, R. Kinsler, and G. Moss, "Data Acquisition for Armored Vehicle Components: Part I, Control Rods," BRL Report (in preparation).*

[3] *C. Zener, "The Micro-mechanism of Fracture," Fracturing of Metals, F. Jonassen, W. Roop, and R. Baylees, Eds., American Society for Metals, Metals Park, Ohio, 1948, pp. 3-31.*

[4] *R. F. Recht, "Catastrophic Thermoplastic Shear," J. Appl. Mech., Paper No. 63-WA-67, November 1963, pp. 1-5.*

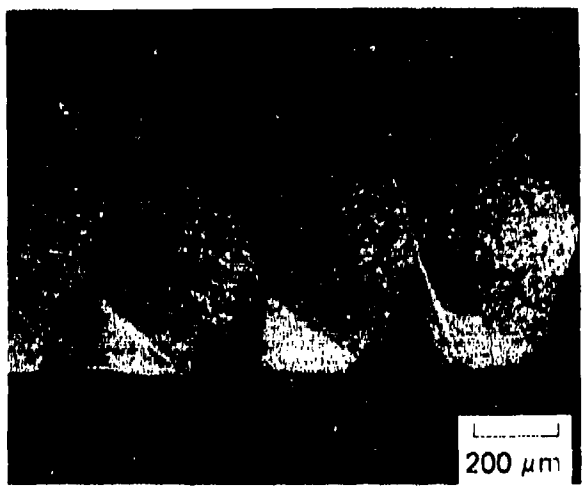

1a

1b

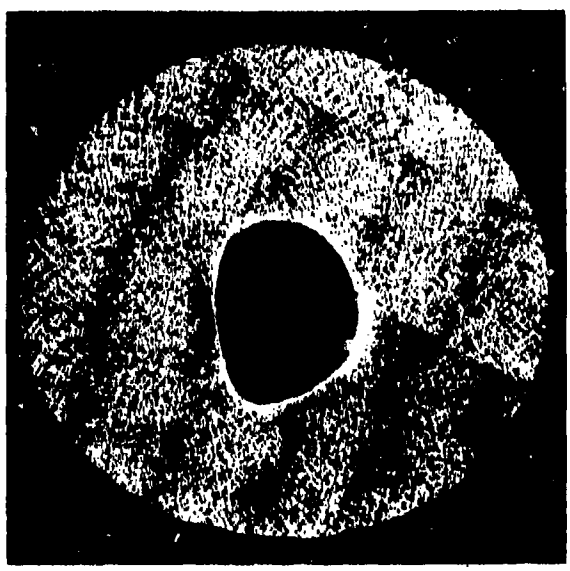

1c

Figure 1. Examples of adiabatic shear bands formed in three different materials. (a) Machining chips of 4340 steel (R_c 40) formed by cutting 1.07mm deep at 0.26 m/sec. The narrow light bands along the nearly vertical interfaces between the chips, as well as the somewhat broader bands at approximately 65° are the adiabatic shear bands.[1] (b) 52100 steel ball bearing (R_c 63) after impact on annealed 1020 steel at 1830 m/sec. The narrow light bands in the dark matrix are the adiabatic shear bands.[2] (c) Aluminum alloy rod after radial explosive compression with Composition B. The shear bands are the approximately logarithmic spirals.

In the course of developing an experiment to determine a consistent set of data, i.e., T, W (the width of an adiabatic shear band), γ and $\dot{\gamma}$, to evaluate shear band models, it was discovered that the microstructure of the Ni-Cr steel being investigated could be used to establish the shear strain γ within the adiabatic shear bands formed in this material.

Once the shear strains in the shear bands were determined, a method of determining the shear strain rates within the shear bands became apparent.

In the following, the methods of determing the shear strain and strain rates of adiabatic shear bands will be described along with values observed for the Ni-Cr steel.

II. EXPERIMENTAL APPROACH

Planar adiabatic shear bands were created with explosive loading as shown in Fig. 2. With the system shown, an appreciable fraction of the explosive energy is absorbed by the momentum trap which, in turn, drives the square-ended punch through the sample. The momentum trap serves to attenuate the stress waves created with the explosion. This is important in creating a reasonably continuous, although rapid, shear as opposed to deformation involving repetitive pulsing by intense stress waves.

It was observed that the buffer did not spall at the end opposite the explosive. Since the nucleation threshold stress of alpha iron is 0.3 GPa[5] it is clear that the intensity of the stress waves transmitted to the sample through the buffer and the punch were substantially less than 0.3 GPa. Hence, shock compression and heating of the target was negligible.

The steel punch was hardened to Rockwell C 52 and had a square cross section. These conditions resulted in approximately flat shear surfaces - a condition required for the determination of the shear strain and strain rate.

The Ni-Cr steel in which the plastic shear was investigated was rolled homogeneous steel armor with the composition given in Table I. The microstructure was bainitic and heavily banded as shown in Fig. 3. The bands were planar chemical inhomogeneities that had been spread through the plate as it was rolled from an ingot. They were extraordinarily plane and parallel with the flat surfaces of the disc shaped sample. These will be referred to as reference bands in the following.

---

[5] *T. W. Barbee, Jr., L. Seaman, R. Crewdson, and D. Curran, "Dynamic Fracture Criteria for Ductile and Brittle Metals," J. Materials, Vol. 7, No. 3, 1972, pp. 393-401.*

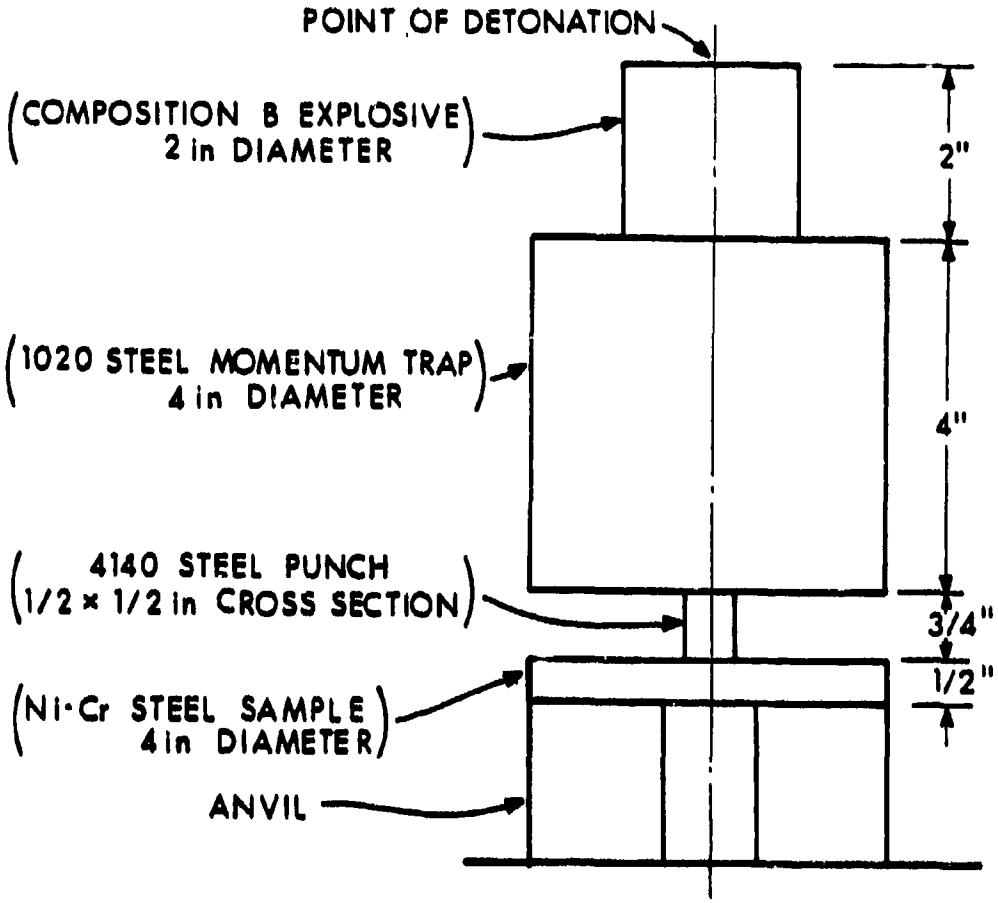

Figure 2. Explosive loading configuration used to create planar shear bands.

TABLE I

COMPOSITION OF STEEL, WEIGHT PERCENT

C	Mn	P	S	Si	Ni	Cr
0.22	0.26	0.001	0.015	0.19	3.15	1.06
Cu	V	Mo	Al	B	Ti	
0.1	0.01	0.15/0.30	0.03	N.D.	N.D.	

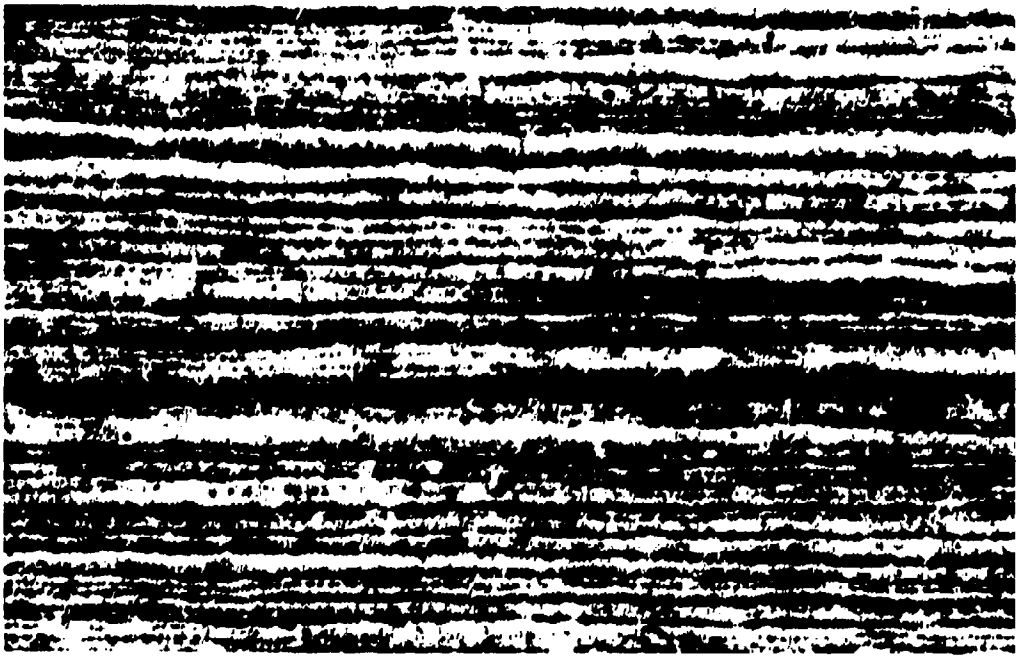

Figure 3. Bands of Chemical Inhomogeneity in the Steel. Stead's etch, X140.

It has been found that when bainitic and martensitic steels are sheared adiabatically, a layer of material within the shear zone is altered and appears light after polishing and etching with certain solutions. The structure of these zones has been investigated on several occasions, but with the purpose of explaining why they appear light after etching. This feature of the shear zones first led to the belief that the "white" layers are martensitic, and subsequent hardness measurements as well as X-ray and electron diffraction records,[6,7] have partially corroborated this point of view, but the martensite is heavily dislocated and could be a new or modified type.

---

[6] *A. L. Wingrove, "A Note on the Structure of Adiabatic Shear Bands in Steel," J. Australian Inst. Metals, Vol. 16, No. 1, 1971, p. 67.*

[7] *R. C. Glenn and W. C. Leslie, "The Nature of White Streaks in Imported Steel Armor Plate," Met. Trans., Vol. 2, 1971, p. 2945-7.*

While contemplating ways that could be used in this program to characterize the shear strain, strain rate and heating of adiabatic shear bands, it was considered possible that the material adjacent to the shear bands would quench them quickly enough after the plug was punched through the plate to allow little chance for the banded structure to be destroyed by alloy diffusion. If this were the situation, the bands of chemical inhomogeneity that existed before deformation should still exist afterwards, but with a shape dependent on the shear. Then, provided they were observable, the chemical inhomogeneities (reference bands) within adiabatic shear bands should serve as "frozen-in" records of the total shear strain developed in the adiabatic shear bands as they formed.

On investigating the microstructure of the shear bands after etching, it was discovered that the chemical inhomogeneities within the shear bands were readily observable in some places. An example is shown in Fig. 4 where it can be seen that the bands of chemical inhomogeneity (reference bands) in the main part of the material extend without disruption into the shear band which is the light region at the edge of the sample. In the vicinity of the shear band, the reference bands bend away from the plane of the plate (horizontal), and they rapidly approach the vertical within the shear band. This change in orientation resulted from the plastic shear of the sample during punching.

If it is assumed that a plate punched by the method shown in Fig. 2 is only sheared and not stretched, it follows that the slope of a reference band at any point on the band is a measure of the strain at that point since the reference bands were originally parallel to the flat surfaces of the plate. The slopes of the reference bands were, therefore, used as a measure of the shear strain within the shear bands.

An Independent measurement of the rate of plugging was required to establish the shear strain rate within the adiabatic shear bands. This was obtained with electrical switches (pins) placed in the path of the plug punched from a sample loaded as shown in Fig. 2.

III. RESULTS

A. Punching Rate During Adiabatic Shearing:

The measurements of the rate of punching revealed a period in which the plug accelerated from rest to a final velocity which was attained in approximately 100 μsec. After this and throughout the remaining time interval in which measurements were made (approximately 525 μsec), the plug moved with a constant velocity.

The measurements indicating this are shown in Fig. 5 where it can be seen that the straight line through the data for times greater than approximately 100 μsec. does not extend through the earlier measurements.

Figure 4. Shear strain revealed within an adiabatic shear band by the deformed bands of chemical inhomogeneity that extend without disruption into the adiabatic shear band from the material to the left. The adiabatic shear band is the relatively white vertical zone at the right edge of the sample. Nital etch, X728.

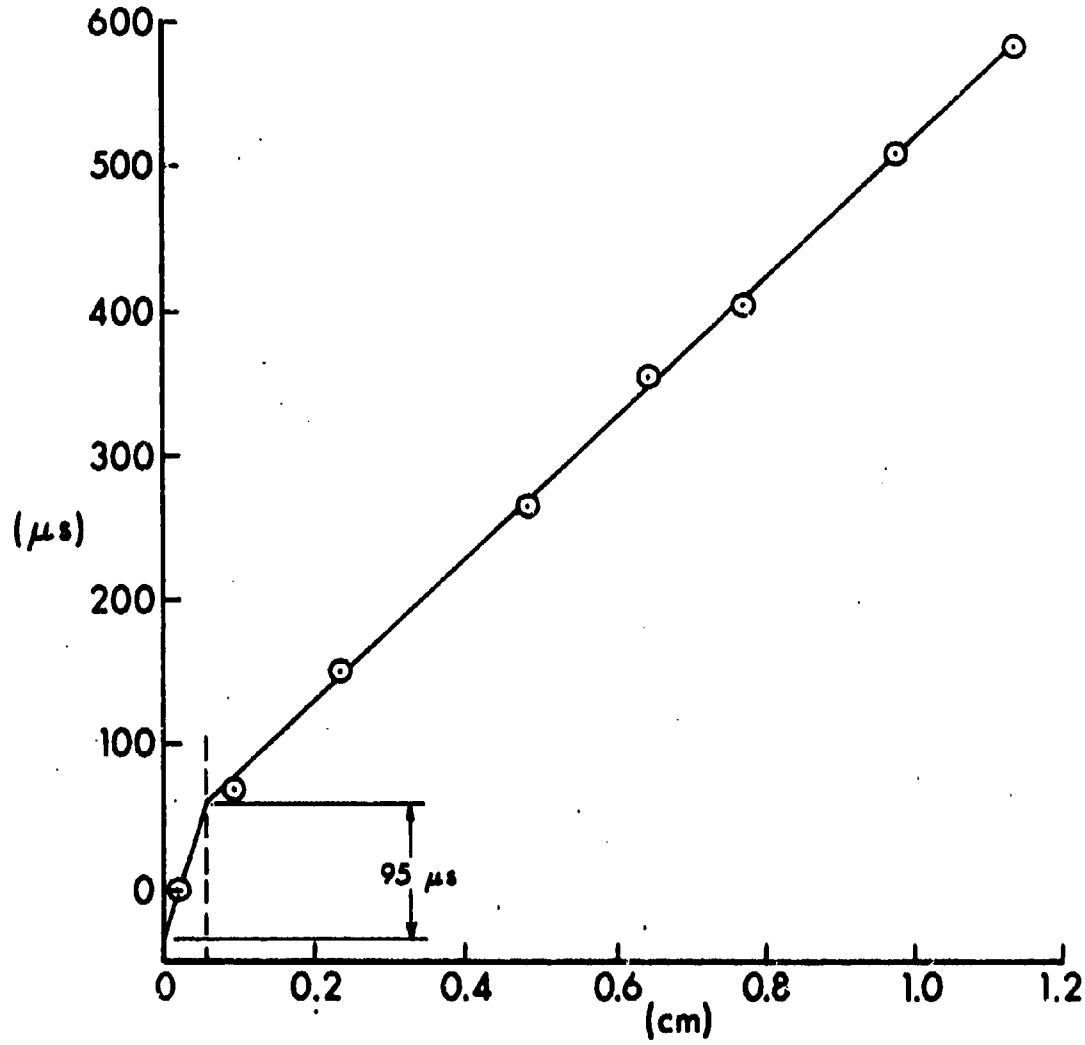

Figure 5. Free surface displacement of a plug sheared from a plate of Ni-Cr steel loaded as shown in Fig. 2.

This is the condition that clearly identifies the initial period of acceleration; however, there is too little data during the period of acceleration to see how the terminal velocity was attained.

The reference bands can be used to determine approximately when the constant velocity region is reached as well as the approximate plugging rate as adiabatic shear occurred. This information is available because once the adiabatic shear band is nucleated, further

deformation is concentrated - at least partly because of thermal softening - within the adiabatic shear bands.

If deformation is concentrated within the adiabatic shear bands, the material adjacent to the shear band must not deform simultaneously. Hence, the reference bands in the material adjacent to the adiabatic shear band becomes a "frozen-in" record of the strain distribution at the time adiabatic shearing began.

The total displacement d of the plug with respect to the rest of the sample at the time an adiabatic shear band nucleates is therefore

$$d = 2\int_0^{w/2} \gamma_x(x)\, dx, \qquad (2)$$

where γ_x is the slope of the reference bands, x is the distance - measured in the plane of the sample - from the center of the plug to a point P on the reference band, and w is the width of the plug. The factor of two enters because there is a shear displacement on both sides of the adiabatic shear band. The displacement and other terms are shown in Fig. 6.

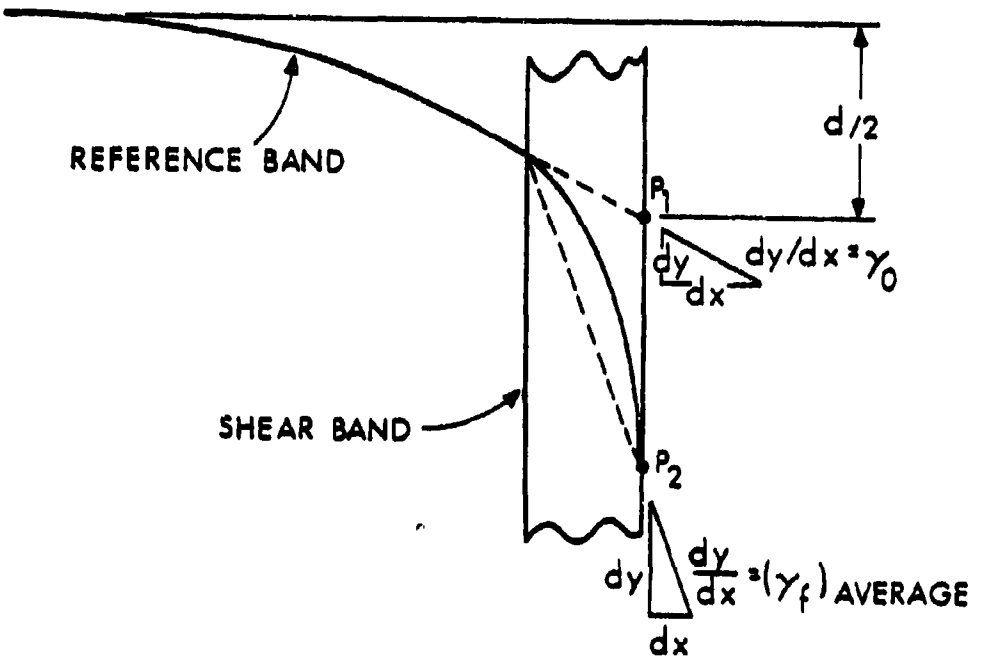

Figure 6. Illustration to describe notation and identify the average shear strain in an adiabatic shear band.

A typical value measured for the displacement d was 0.047 cm, and this has been located on Fig. 5 where it can be seen that the constant velocity region extends almost to this value of x. The exact lower bound on the constant velocity region is unknown because no data was obtained between 0.020 and 0.095 cm. However, it is clear that when the adiabatic shear band nucleated, or soon afterwards, the plug velocity had nearly reached the terminal velocity because d is right at the end of the constant velocity region.

It is unlikely that the plug moved with terminal velocity throughout the entire adiabatic shearing process because the material in the shear zone has some strength even though it softens as deformation occurs. However, the strength of the shear zone approaches zero as deformation proceeds, and the plug must move at almost the terminal velocity as it breaks away from the rest of the sample. Prior to this, the terminal velocity is an upper bound to the plug velocity. Here, the plug velocity during the adiabatic shearing process will be equated to the terminal plug velocity. Estimates of shear strain rates in adiabatic shear bands that are based on this assumption are an upper bound on the real values.

B. Shear Strain Rate During Adiabatic Shear:

Between the time an adiabatic shear band is initiated and the time the plug separates from the sample along the shear band, Point P_1 moves to P_2 as shown in Fig. 6. The plugging velocity during the same time interval was, as described above, approximately equal to the final plug velocity v_p so the shear band formed in a time increment $\Delta t = (P_2-P_1)/v_p$.

The average shear strain developed through the thickness of an adiabatic shear band in the time interval Δt during which it formed can be defined as $(\gamma_f-\gamma_o)$ where γ_f and γ_o are rough estimates of the average shear strains throughout the shear band at the end and start of Δt. Clearer descriptions of γ_f and γ_o are given in Fig. 6.

Hence, the average shear strain rate in the adiabatic shear band was

$$\dot{\gamma}_{avg} = \frac{\Delta\gamma_{avg}}{\Delta t} = \frac{(\gamma_f-\gamma_o)_{avg}}{(P_2-P_1)/v_p} \quad . \tag{3}$$

The average shear strain rate determined from a set of typical measurements was 8.77×10^5 sec^{-1}. However, it is immediately apparent on viewing Fig. 4 that the shear strain and, therefore, the strain rate is a strong function of distance through the shear band. The shear strain $\gamma_f(x)$ at a particular location x is readily obtained by measuring the slope at a point of the reference band as suggested in §II.

A graph showing how the shear strain $[\gamma_f(x) - \gamma_o(x)]$ resulting from adiabatic shear varied with distance through a shear band is shown in Fig. 7. $\gamma_o(x)$ is the shear strain at location x at the time the shear band started to form. These initial strains were estimated from extrapolations of the reference bands adjacent to the adiabatic shear bands.

If it is assumed that the shear strain at each location develops continuously over the time interval Δt during which the band forms, the shear strain rate at location x is given by

$$\dot{\gamma}(x) = \frac{\gamma_f(x) - \gamma_o(x)}{\Delta t} \quad . \tag{4}$$

Strain rates corresponding to the strains shown in Fig. 7 and estimated according to Eq. 4 are shown in Fig. 8. It is apparent that maximum shear strain rates as large as 9.4×10^7 sec.$^{-1}$ occurred.

IV. DISCUSSION

Within a distance of 4×10^{-4} cm from the surface where the plug separated from the rest of the sample, the reference bands were usually not resolvable. They were indistinguishable in this region because they were disrupted beyond recognition by plastic deformation and whatever recovery may have followed. It is apparent because of the lack of resolution that the strain was greater here than anywhere else in the sample. Hence, at the plane of separation, shear strains greater than 572 must have been attained.

In computing $\dot{\gamma}(x)$, it was assumed that the strain rate at x is the same throughout the time interval during which a shear band forms, but because of thermal softening, successive deformation may tend to concentrate in an ever decreasing region of a shear band. If this actually occurs, the shear strain rates shown in Fig. 8, must be lower bounds on the actual values.

The temperature change in an infinite solid at a distance x from the center of a region of width 2a in which heat is generated at a rate $\dot{Q}(x,t_1)$ is given by

$$\Delta T(x,t) = \int_o^t \frac{1}{2\sqrt{\pi k(t-t_1)}} \int_o^\infty \dot{Q}(x,t_1) \left[e^{\frac{-(x-x^1)^2}{4k(t-t_1)}} + e^{\frac{-(x+x^1)^2}{4k(t-t_1)}} \right] dx^1 dt_1, \tag{5}$$

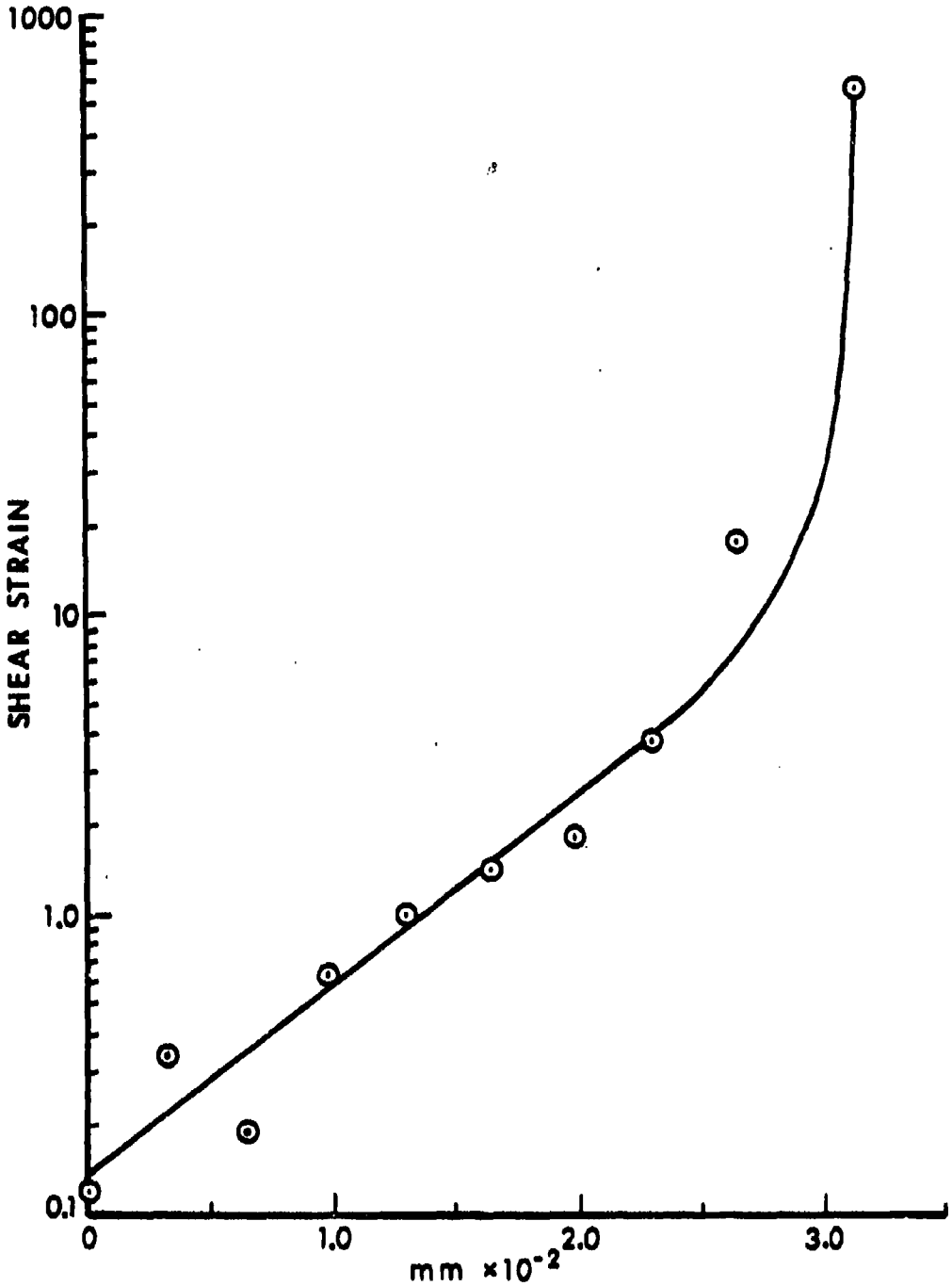

Figure 7. Shear strain $[\gamma_f(x) - \gamma_o(X)]$ versus distance through an adiabatic shear band.

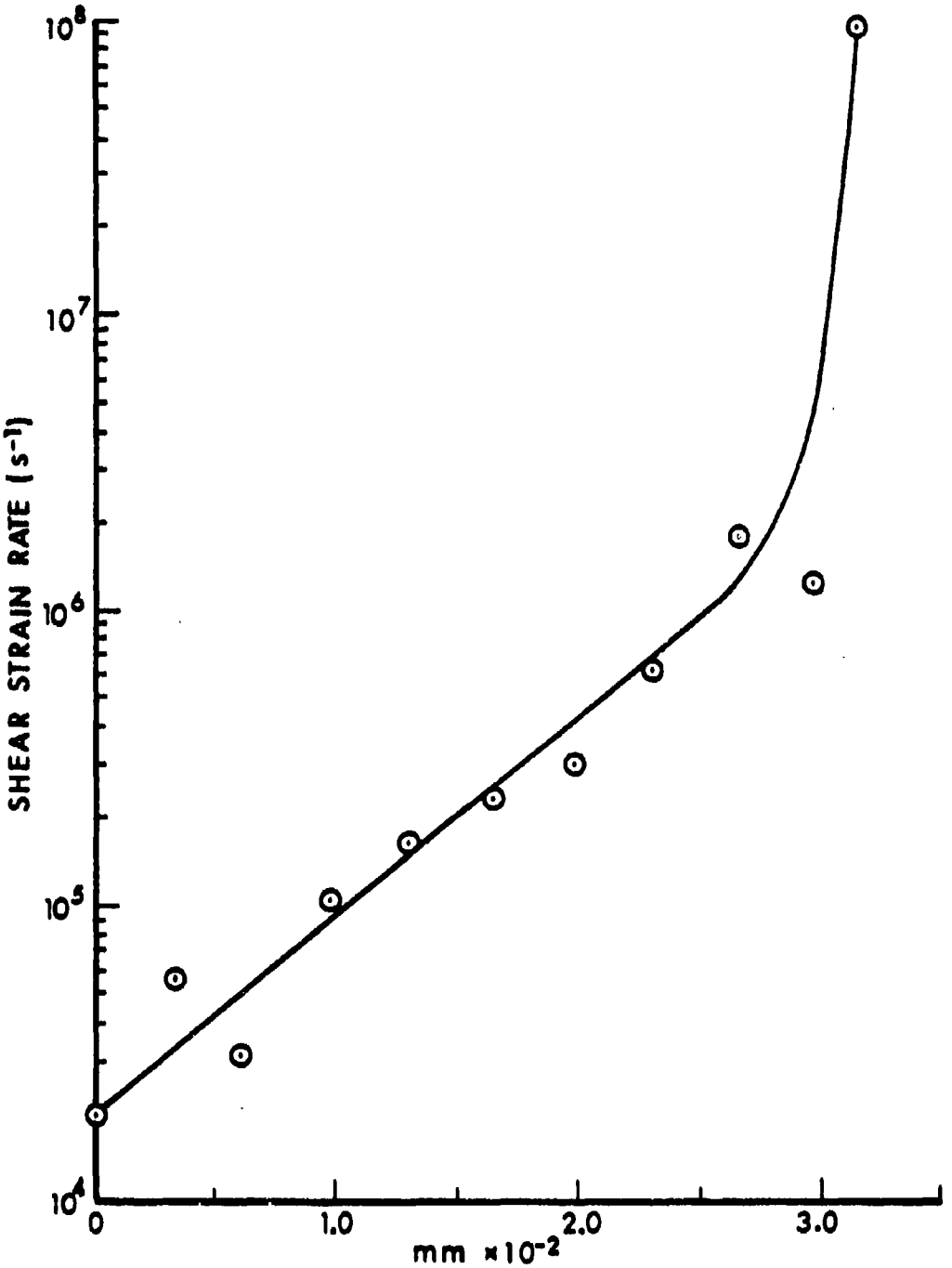

Figure 8. Shear strain rate $[\gamma_f(x) - \gamma_o(x)]/\Delta t$ versus distance through an adiabatic shear band.

where k is the diffusivity of the material and t is the time since heating began.[8] The pair of exponential terms insure no heat transfer across the plane of symmetry.

The experimental observation has been that the plastic strain rate in the adiabatic shear band is approximately given by the relation

$$\ln \dot{\gamma} = -mx+b, \tag{6}$$

where b is the intercept, $\ln \dot{\gamma}_o$, and (-m) is the slope of the straight line portion of the curve in Fig. 8. The slope is negative because the origin of the x axis was taken at the plane of separation. Hence, the rate of plastic working in the shear zone is also a function of x, and the heating rate is given by

$$\dot{Q} = \frac{\tau f \dot{\gamma}_o e^{-mx}}{JC\rho} \quad , \quad o \leq x \leq a$$
$$= 0 \quad , \quad a < x < \infty \tag{7}$$

where τ is the flow stress, and f is the fraction of the mechanical work converted to heat.

In previous attempts to model the heating from plastic work in adiabatic shear bands, it has been assumed that $\dot{Q}$ is the same throughout the shear band and is independent of time. For this situation, $\dot{Q}$ is a constant and can be taken outside the integrals of Eq. 4, but this certainly cannot be done when conditions are analogous to those described here.

Since the heating rate $\dot{Q}$ has been determined as a function of distance through a shear band, meaningful temperature computations are now possible. However, before describing such a computation, it is useful to consider the maximum possible temperature changes within the adiabatic shear band. Such an upper bound can be determined by assuming 100 percent conversion of plastic work to heat, no thermal softening and no conduction. These temperatures are shown in Fig. 9.

Certainly, temperatures substantially greater than the melting point, as shown near the plane of separation, would never be attained because liquids can be sheared with much lower stresses than solids. However, it is suggested that melting is possible, and observations of

[8] *H. S. Carslaw and J. C. Jaeger, Conduction of Heat in Solids, Oxford University Press, London, 1959.*

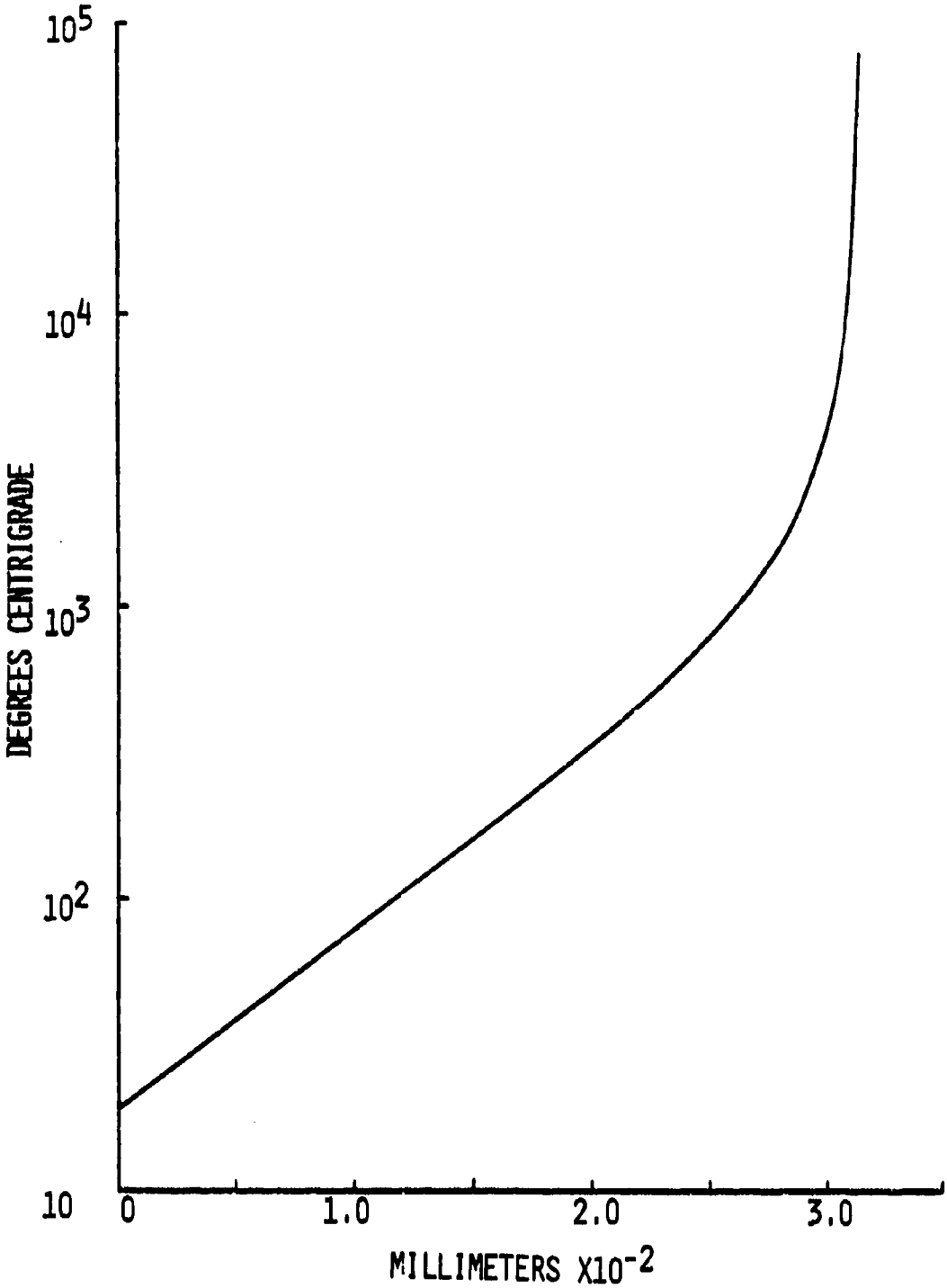

Figure 9. Maximum temperature changes in an adiabatic shear band. Temperature change computed by assuming 100 percent conversion of plastic work to heat and no heat conduction.

sheared surfaces with scanning electron microscopy[9] and the temperature measurements of Bowden[10] support this point of view.

Since during deformation the maximum temperature at the location in the shear band where $d(\ln \gamma)/dx$ changes abruptly was way below the melting point of the steel (Fig. 9), the change in slope may have been due to a solid-state transformation. It would be worth knowing if such a transformation were related to the slope change since, if it were, it would be equally responsible for the constriction of plastic flow between γ_{cr} (the strain at the slope change in Fig. 7) and the plane of separation. The constricted flow must have occurred because the velocity of the plug during adiabatic shear was about constant according to Fig. 5. With this condition, an increase in strain rate in one part of the band--a possibility according to Fig. 8--necessitates a decrease in velocity somewhere else.

A test of whether or not the transition strain γ_{cr} was related to a solid-state transformation can be made by computing the related temperature change to establish whether or not it equals the temperature at which a solid-state transformation could be expected to start. In pursuit of such a test, a computation of the temperature corresponding to γ_{cr} will be described next.

For strains up to γ_{cr}, the heating rate throughout the entire shear band should be given by the nonzero part of Eq. 7 provided the change in slope of the $\ln \gamma$-x curve developed after γ_{cr} was reached. This is the situation that has already been described as likely.

While there may not have been any heating outside the adiabatic shear band as it formed, the heating will be treated as though the first part of Eq. 7 applied throughout the sample. Even though this allows heating outside the bounds of the adiabatic shear band, conditions are approximated reasonably well because of the exponential form of Eq. 7. Furthermore, prior to the formation of the adiabatic shear band, there was plastic deformation and heating over a broad region bounding the final location of the adiabatic shear band as shown in Fig. 4. Hence, allowing some heating outside the region of the shear band as it forms partly compensates for the initial temperature distribution.

The conditions described can be restated more succinctly as the region $x>o$ initially at T_o subjected to heating given by $A \exp(-mx)$ for $t>o$ and no conduction across the plane $x=o$. The temperature $T(x,t)$ is given by[11]

---

[9] *T. A. C. Stock and K. R. L. Thompson, Met. Trans., 1, 1970, p. 219.*

[10] *F. P. Bowden and P. H. Thomas, "The Surface Temperature of Sliding Solids," Proc. Roy. Soc., Ser. A, Vol. 233, 1954, pp. 29-40.*

[11] *H. S. Carslaw and J. C. Jaeger, op. cit.*

$$T(x,t) = T_o + \frac{2A}{Km}(kt)^{\frac{1}{2}}\ \text{ierfc}\ \frac{x}{2(kt)^{\frac{1}{2}}} - \frac{A}{m^2k}\ e^{-mx} +$$

$$+ \frac{A}{2Km^2}\ e^{m^2kt-mx}\ \text{erfc}\left[m(kt)^{\frac{1}{2}} - \frac{x}{2(kt)^{\frac{1}{2}}}\right] + \qquad (8)$$

$$+ \frac{A}{2km^2}\ e^{m^2kt+mx}\ \text{erfc}\left[m(kt)^{\frac{1}{2}} + \frac{x}{2(kt)^{\frac{1}{2}}}\right],$$

where $A = \tau f\dot{\gamma}_o/J$. The computation is simplified by finding the temperature $T(o,t_{cr})$ at x=o when γ reaches γ_{cr}. This happens in a time interval $t_{cr} = \gamma_{cr}/\dot{\gamma}_o$. $T(o,t_{cr})$ is given by

$$T(o,t_{cr}) = T_o + \frac{2A}{Km}\ (kt_{cr})^{\frac{1}{2}}\ \text{ierfc}\ 0 - \frac{A}{m^2K}\left[1-e^{m^2kt_{cr}}\ \text{erfc}\ m(kt_{cr})^{\frac{1}{2}}\right]. \qquad (9)$$

The thermal properties of steel are a function of composition; hence, a computation of $T(o,t_{cr})$ for the adiabatic shear that has been described was based on the thermal properties of a tempered martensitic 0.34 C, 3.53 Ni, 0.78 Cr steel--a steel with nearly the same composition as the steel on which the shear tests were performed.[12] Strains as great as γ_{cr} are clearly sufficient, according to Fig. 9, to cause substantial temperature changes, but the thermal conductivity K and diffusivity k change with temperature. Hence, average values over the temperature range $T_o<T<T(o,t_{cr})$ were used in computing $T(o,t_{cr})$. Since $T(o,t_{cr})$ was not initially known, the average values for k and K were determined iteratively.

With this approach and data, $T(o,t_{cr}) = T_{cr}$ was determined to be 531°C. The average values determined for k and K were 0.0796 cm^2/sec and 0.0849 cal/cm sec°C, respectively.

Solid-state transformations that occur in steel at temperatures near T_{cr} are listed in Table II.

---

[12] *Metals Handbook, Ninth Edition, Vol. 1, Ed. Bruce P. Bardes, American Society for Metals, Metals Park, Ohio, 1978, pp. 148-9.*

TABLE II

SOLID-STATE TRANSFORMATIONS IN BAINITIC STEEL

TRANSFORMATION	TRANSFORMATION TEMPERATURE, °C
Bainite → γ Fe	Approximately 690
Bainite → α Fe + Fe_3C	538 (Strain Dependent)
Magnetic Change	Approximately 500-670

Only the carbon and nickel in the steel investigated would appreciably affect the temperature at which gamma iron (γ Fe) forms. With carbon, iron undergoes the well-known eutectoid reaction which starts at 723°C while pure iron transforms at 910°C. Nickel lowers the transformation temperature, but the reaction is sluggish and, therefore, not well documented. It has been reported, however, that the nickel in low-carbon steels lowers the eutectoid temperature 10.6°C for each percent nickel added.[13] Hence, the eutectoid temperature of the 3.1 percent nickel steel investigated should be approximately 690°C. Deformation assists some transformations, but it would be more likely to favor the formation of bainite than gamma iron because the γ→ bainite reaction is a shear transformation. Furthermore, the eutectoid temperature of nickel steels is higher on heating than on cooling.[14] Hence, the transformation temperature of 690°C listed in Table II should be a lower bound. This is still 159°C greater than T_{cr} and clearly rules out the transformation of bainite to gamma iron as being responsible for the change in strain gradient in the shear band at γ_{cr}.

The properties of steels are often tailored to a need by tempering a previously hardened product. When the resultant microstructure is bainitic, it is found that it must be reheated to a temperature above the tempering temperature to transform the microstructure to alpha iron (ferrite) and Fe_3C in any short-time anneal.[15] Presumably, heating to just slightly above the tempering temperature results in accelerated bainite decomposition. After T_{cr} was computed, it was established with the manufacturer's records that the steel investigated had been tempered at 538°C. This is only 7 degrees above the computed temperature, and even though plastic deformation could change the short-time transformation temperature, it is concluded that it is highly probable that the formation of ferrite was at least partly responsible for the change in strain gradient at γ_{cr}.

[13] *C. M. Schwitter, Metals Handbook, Ed. Taylor Lyman, American Society for Metals, 1948, p. 1254.*

[14] *Ibid., p. 474.*

[15] *Walter Crafts and John L. Lamont, Hardenability and Steel Selection, Pitman Publishing Corp., New York, 1944, p. 154.*

In addition, the change in specific heat with temperature of the Ni-Cr steel investigated starts to increase drastically with increasing temperature at approximately 500°C, and this could be partly responsible for the change in the strain gradient at γ_{cr}. Of course, an increase in specific heat means that the work required to increase the temperature one degree must also increase. Hence, the increase in d^2C_p/dT^2 that becomes more appreciable at 500°C does not relate to a thermal softening mechanism. Instead, it suggests a magnetic transformation is involved. Since, in the past, this has not been considered to be a factor in adiabatic shear, the way in which it should be influential will be described. The increase in d^2C_p/dT^2 is due to an increase in the randomness of the magnetic structure--electron spin--of the alloy, and this is a type of order→disorder transformation. The magnetic domains are correspondingly disrupted. Normally, the boundaries between ordered regions act as barriers to dislocation motion. Distruction of these boundaries should, therefore, reduce the stress to deform the material. Hence, the magnetic transformation that starts at about 500°C should be a softening mechanism.

The relative effects of the formation of ferrite and the disruption of the magnetic structure of the alloy are not known, but it can be anticipated that both changes are related to the change in strain gradient in the adiabatic shear band at γ_{cr} since they both start at about the same temperature.

The strength of steel as adiabatic shear progresses is unknown, and an assumption about this was necessary before an estimate of T_{cr} could be made. It was assumed that the shear stress equaled half the ultimate tensile strength of the steel at room temperature. If the computed temperature had not equaled any solid-state transformation temperature, it would have been concluded that the assumption about the strength was possibly a poor one. However, it can be concluded from the agreement obtained that there was little thermal softening for shear strains up to 570 percent.

If there were truly no thermal softening, one might want to question why the shear strain should become confined to a narrow band. Apparently, there is some thermal softening, but it is not appreciable. Still, negligible thermal softening while there is substantial heating appears to be a conflicting situation. However, it is also true that thermal softening decreases as strain rate increases,[16] and it is believed that the lack of recognizable thermal softening was a consequence of the extremely high strain rates in the adiabatic shear band.

---

[16] *J. J. Jonas and M. J. Luton, "Flow Softening at Elevated Temperatures,"* Advances in Deformation Processing, *Ed. John J. Burke and Volker Weiss, Plenum Press, New York, 1978, pp. 215-243.*

V. CONCLUSIONS

It has been discovered that the planes of chemical inhomogeneity (reference bands) left from the casting and rolling of steels can be used to document the shear strain in adiabatic shear bands.

These reference bands change shape during plastic deformation according to the orientation of the shear displacements and the amount of plastic shear. When the reference bands are perpendicular to the shear displacements, the slope of the reference band is a direct measure of the plastic shear strain.

In an experiment with a Ni-Cr steel in which this situation could be exploited, the reference bands were used to investigate the plastic deformation within adiabatic shear bands. It was found that the strain varied through the thickness, as well as along the length of a shear band.

The greatest strains occurred near the surfaces where the samples were sheared in-two. The strains near these surfaces were as high as 57,200 percent, while the average shear strain was found to be approximately 530 percent.

The shear bands investigated were created by driving a rigid punch through a plate, and measured rates of plugging, coupled with the measured shear strains, were used in a new determination of shear strain rates within adiabatic shear bands. The average strain rate within the adiabatic shear bands investigated was on the order of 9×10^5 sec^{-1}, but strain rates as high as 9.4×10^7 sec^{-1} were clearly developed near the surfaces where the samples sheared in-two.

The methods that have been developed and described should be useful in establishing quantitative descriptions of adiabatic shear required for the construction and testing of models of dynamic shear failure.

It has been suggested previously that as adiabatic shear bands form in steel there can be a transformation from ferrite to austenite. This, was originally inferred from the white etching nature of shear bands sectioned after deformation. Since austenite is substantially weaker than martensite or bainite, such a transformation in a shear band would amount to substantial weakening. However, it was shown here with a temperature computation that it was a bainite $\rightarrow$ ferrite + Fe_3C and possibly a magnetic transformation that governed the abrupt change in the strain gradient in the adiabatic shear band in the steel investigated.

It was also concluded that thermal softening at the strain rates investigated was not appreciable for strains up to 570 percent.

REFERENCES

1. K. C. Dao and D. A. Shockey, "A Method for Measuring Shear Band Temperatures," J. Applied, Phys., Vol. 50, No. 12, December 1979, pp. 8244-6.

2. W. Braerman, R. Kinsler, and G. Moss, "Data Acquisition for Armored Vehicle Components: Part I, Control Rods," BRL Report (in preparation).

3. C. Zener, "The Micro-mechanism of Fracture," Fracturing of Metals, F. Jonassen, W. Roop, and R. Bayless, Eds., American Society for Metals, Metals Park, Ohio, 1948, pp. 3-31.

4. R. F. Recht, "Catastrophic Thermoplastic Shear," J. Appl. Mech., Paper No. 63-WA-67, November 1963, pp. 1-5.

5. T. W. Barbee, Jr., L. Seaman, R. Crewdson, and D. Curran, "Dynamic Fracture Criteria for Ductile and Brittle Metals," J. Materials, Vol. 7, No. 3, 1972, pp. 393-401.

6. A. L. Wingrove, "A Note on the Structure of Adiabatic Shear Bands in Steel," J. Australian Inst. Metals, Vol. 16, No. 1, 1971, p. 67.

7. R. C. Glenn and W. C. Leslie, "The Nature of White Streaks in Imported Steel Armor Plate," Met. Trans., Vol. 2, 1971, p. 2945-7.

8. H. S. Carslaw and J. C. Jaeger, Conduction of Heat in Solids, Oxford University Press, London, 1959.

9. T. A. C. Stock and K. R. L. Thompson, Met. Trans., 1, 1970, p. 219.

10. F. P. Bowden and P. H. Thomas, "The Surface Temperature of Sliding Solids," Proc. Roy. Soc., Ser. A, Vol. 233, 1954, pp. 29-40.

11. H. S. Carslaw and J. C. Jaeger, op. cit.

12. Metals Handbook, Ninth Edition, Vol. 1, Ed. Bruce P. Bardes, American Society for Metals, Metals Park, Ohio, 1978, pp. 148-9.

13. C. M. Schwitter, Metals Handbook, Ed. Taylor Lyman, American Society for Metals, 1948, p. 1254.

14. Ibid., p. 474.

15. Walter Crafts and John L. Lamont, Hardenability and Steel Selection, Pitman Publishing Corp., New York, 1944, p. 154.

16. J. J. Jonas and M. J. Luton, "Flow Softening at Elevated Temperatures," Advances in Deformation Processing, Ed. John J. Burke and Volker Weiss, Plenum Press, New York, 1978, pp. 215-243.

DISTRIBUTION LIST

No. of Copies	Organization
12	Commander Defense Technical Info Center ATTN: DDC-DDA Cameron Station Alexandria, VA 22314
2	Director Defense Advanced Research Projects Agency ATTN: Tech Info Dr. Ernest F. Blase Dr. Bement Dr. Ray Gogolewski 1400 Wilson Boulevard Arlington, VA 22209
1	Deputy Assistant Secretary of the Army (R&D) Department of the Army Washington, DC 20310
1	Commander US Army War College ATTN: Lib Carlisle Barracks, PA 17013
1	Commander US Army Command and General Staff College ATTN: Archives Fort Leavenworth, KS 66027
1	Commander US Military Academy ATTN: Library West Point, NY 10996
1	Commander US Army Materiel Development & Readiness Command ATTN: DRCDMD-ST 5001 Eisenhower Avenue Alexandria, VA 22333
6	Commander US Army Armament Research & Development Command ATTN: DRDAR-TSS (2 cys) J.D. Corrie R.J. Weimer J. Beetle E. Bloore Dover, NJ 07801
1	Commander US Army Armament Materiel Readiness Command ATTN: DRSAR-LEP-L, Tech Lib Rock Island, IL 61299
1	Director US Army ARRADCOM Benet Weapons Laboratory ATTN: DRDAR-LCB-TL Watervliet, NY 12189
5	Commander US Army Watervliet Arsenal ATTN: Dr. T. Davidson Dr. M.A. Hussain Dr. S.L. Pu Mr. D.P. Kendall Dr. John Underwood Watervliet, NY 12189
1	Commander US Army Aviation Research & Development Command ATTN: DRSAV-E P.O. Box 209 St. Louis, MO 63166
1	Director US Army Air Mobility Research & Development Laboratory Ames Research Center Moffett Field, CA 94035

DISTRIBUTION LIST

No. of Copies	Organization
1	Commander US Army Communications Research & Development Command ATTN: DRDCO-PPA-SA Fort Monmouth, NJ 07703
1	Commander US Army Electronics Research & Development Command Technical Support Activity ATTN: DELSD-L Fort Monmouth, NJ 07703
1	Commander US Army Harry Diamond Labs ATTN: DRXDO-TI 2800 Powder Mill Road Adelphi, MD 20783
3	Commander US Army Missile Command ATTN: DRDMI-R DRDMI-YDL Dr. Raymond Conrad Redstone Arsenal, AL 35809
3	Commander US Army Mobility Equipment Rsch & Development Command ATTN: DRDME-WC DRSME-RZT STSFB-MW, Dr.J. Bond Fort Belvoir, VA 22060
1	Commander US Army Tank Automotive Rsch & Development Command ATTN: DRDTA-UL Warren, MI 48090
5	Commander US Army Materials and Mechanics Research Center ATTN: DRXMR-ATL DRXMR-H, Dr.D. Dandekar DRXMR-T, Mr.J. Mescall DRXMR-H, Dr.S.C. Chou Watertown, MA 02172
3	Commander US Army Research Office ATTN: Dr. Hermann Robl Dr. E. Sailbel Dr. George Mayer Dr. James Murray P.O. Box 12211 Research Triangle Park NC 27709
1	Commander US Army Research & Standardization Group (Europe) ATTN: Dr. B. Steverding Box 65 FBO NY 09510
1	Director US Army TRADOC Systems Analysis Activity ATTN: ATAA-SL, Tech Lib White Sands Missile Range NM 88002
1	Office of Naval Research ATTN: Code 402 Department of the Navy 800 N. Quincy Street Arlington, VA 22217
2	Commander Naval Surface Weapons Center ATTN: Mr. W.H. Holt DX-21, Lib Dahlgren, VA 22445

DISTRIBUTION LIST

No. of Copies	Organization
2	Commander Naval Surface Weapons Center ATTN: Dr. Robert Crowe Tech Lib Silver Spring, MD 20910
1	Commander Naval Research Laboratory ATTN: Code 2020, Tech Lib Washington, DC 20375
7	Commander Naval Research Laboratory Engineering Materials Division ATTN: E.A. Lange G.R. Yoder C.A. Griffis R.J. Goode R.W. Judy, Jr. A.M. Sullivan T.W. Crooker Washington, DC 20375
1	Commander Naval Research Laboratory Metallurgy Division ATTN: W.S. Pellini Washington, DC 20375
1	AFOSR (Dr. Alan H. Rosenstein) Bolling AFB, DC 20332
1	AFWL (Tech Lib) Kirtland AFB, NM 87117
1	Director Lawrence Livermore Laboratory ATTN: Dr.M.L. Wilkins P.O. Box 808 Livermore, CA 94550
5	Sandia Laboratories ATTN: Tech Lib Dr. A.L. Stevens Dr. Lee Davison Dr. W.E. Warren Dr. L.D. Bertholf Dr. Marlin Kipp Albuquerque, NM 87115
1	Terra Tek, Inc. ATTN: Dr. Arfon Jones 420 Wahara Way University Research Park Salt Lake City, UT 84108
1	Brown University Division of Applied Mathematics ATTN: Prof. H. Kolsky Providence, RI 02912
2	Brown University Division of Engineering ATTN: Prof. James R. Rice Prof. L.B. Freund Providence, RI 02912
1	Colorado School of Mines Dept of Metallurgical Engr ATTN: Prof. George Krauss Golden, CO 80401
1	Drexel University Dept of Materials Engineering ATTN: Prof. Harry C. Rogers Philadelphia, PA 19104
2	The Johns Hopkins University ATTN: Prof. R.B. Pond, Sr. Prof. R. Green 34th and Charles Streets Baltimore, MD 21218

DISTRIBUTION LIST

No. of Copies	Organization
1	Lehigh University Institute of Fracture and Solid Mechanics ATTN: Prof. George C. Sih Bethleheml, PA 18015
1	Lehigh University Department of Mechanics ATTN: Prof. Frazil Erdogen Bethlehem, PA 18015
1	Louisiana State University ATTN: Prof. W.N. Sharpe, Jr. Baton Rouge, LA 70803
1	Massachusetts Inst of Tech ATTN: Prof. Frank A. McClintock 77 Massachusetts Avenue Cambridge, MA 02139
1	Michigan Technological Univ Dept of Metallurgical Engr. ATTN: Prof. Dale F. Stein Prof. Donald E. Mikkola Houghton, MI 49931
1	South Dakota State University Dept of Mechanical Engineering ATTN: Prof. Michael P. Wnuk Brookings, SD 57006
4	SRI International ATTN: Dr. Goerge R. Abrahamson Dr. Donald R. Curran Dr. Donald A. Shockey Dr. Lynn Seaman 333 Ravenswood Avenue Menlo Park, CA 94025
2	University of California Los Alamos Scientific Lab ATTN: Dr.W.E. Deal, Jr. Tech Lib P.O. Box 1663 Los Alamos, CA 87545
1	University of Illinois Department of Theoretical and Applied Mechanics College of Engineering ATTN: Prof. Herbert T. Corten Urbana, IL 61801
1	University of Notre Dame Dept of Metallurgical Engineering and Materials Sciences ATTN: Prof. N.F. Fiore Notre Dame, IN 46556
1	University of Pittsburgh ATTN: Dean M.L. Williams Pittsburgh, PA 15261
1	University of Washington Department of Mechanical Engineering ATTN: Prof. A.S. Kobayashi Seattle, WA 98105
1	Union College ATTN: Prof. Raymond Eisenstadt Schenectady, NY 12308
1	Washington State University Department of Physics ATTN: Prof. G.E. Duvall Pullman, WA 99163
	Aberdeen Proving Ground
	Dir, USAMSAA ATTN: DRXSY-D DRXSY-MP, H. Cohen
	Cdr, USATECOM ATTN: DRSTE-TO-F
	Dir, Wpns Sys Concepts Team Bldg E3516, EA ATTN: DRDAR-ACW

USER EVALUATION OF REPORT

Please take a few minutes to answer the questions below; tear out this sheet and return it to Director, US Army Ballistic Research Laboratory, ARRADCOM, ATTN: DRDAR-TSB, Aberdeen Proving Ground, Maryland 21005. Your comments will provide us with information for improving future reports.

1. BRL Report Number _____

2. Does this report satisfy a need? (Comment on purpose, related project, or other area of interest for which report will be used.)

_____

_____

_____

3. How, specifically, is the report being used? (Information source, design data or procedure, management procedure, source of ideas, etc.) _____

_____

_____

4. Has the information in this report led to any quantitative savings as far as man-hours/contract dollars saved, operating costs avoided, efficiencies achieved, etc.? If so, please elaborate.

_____

_____

5. General Comments (Indicate what you think should be changed to make this report and future reports of this type more responsive to your needs, more usable, improve readability, etc.) _____

_____

_____

_____

6. If you would like to be contacted by the personnel who prepared this report to raise specific questions or discuss the topic, please fill in the following information.

Name: _____

Telephone Number: _____

Organization Address: _____

_____

_____